Nano Energy (2013) 2, 764–768

Available online at www.sciencedirect.com

ScienceDirect

journal homepage: www.elsevier.com/locate/nanoenergy

RAPID COMMUNICATION

Volumetric capacitance of compressed activated microwave-expanded graphite oxide (a-MEGO) electrodes

Shanthi Murali[a], Neil Quarles[a], Li Li Zhang[a], Jeffrey R. Potts[a], Ziqi Tan[b], Yalin Lu[b], Yanwu Zhu[b,*], Rodney S. Ruoff[a,*]

[a]*Department of Mechanical Engineering and the Materials Science and Engineering Program, The University of Texas at Austin, One University Station C2200, Austin, TX 78712, United States*
[b]*Department of Materials Science and Engineering and the CAS Key Laboratory of Materials for Energy Conversion, University of Science and Technology of China, Hefei 230026, China*

Received 24 October 2012; received in revised form 15 January 2013; accepted 15 January 2013
Available online 7 February 2013

KEYWORDS
Graphene;
Pore size;
Supercapacitors;
Volumetric capacitance;
Organic electrolyte;
Compression;
a-MEGO

Abstract
Volumetric capacitance is an important parameter for device applications. By simply compressing activated microwave-expanded graphite oxide (a-MEGO)-based electrode material, a volumetric capacitance of up to 110 F/cm^3 (3.5 V maximum voltage) was achieved, when measured in a two-electrode cell supercapacitor configuration in an organic electrolyte. Nitrogen adsorption showed that the mesopores of a-MEGO (~4 nm) collapsed due to the compression, and more micropores (1–2 nm) contributed to the energy storage in the compressed electrodes compared to uncompressed electrodes. This change in pore structure resulted in a higher effective series resistance and thus reduced power density in the compressed samples.

Introduction

Supercapacitors (electrochemical double layer capacitors; EDLCs) store electrical charge because of the separation of opposite charges at the interface formed between an electrode and an electrolyte [1]. Compared to batteries, supercapacitors have faster charge/discharge rates but store less energy. In an effort to increase the energy storage density of supercapacitors while maintaining or even improving their power output, carbon electrode materials such as activated carbons [2], carbon onions [3], carbide-derived carbons (CDCs) [4], carbon nanotubes [5], and recently graphene-based materials [6], have been intensively studied. In the literature, the electrode performance of supercapacitors-including the specific capacitance, energy, or power-is usually quoted on a gravimetric basis (i.e., per unit weight of the active materials). However, the volumetric

*Corresponding authors.
E-mail addresses: zhuyanwu@ustc.edu.cn (Y. Zhu), r.ruoff@mail.utexas.edu (R.S. Ruoff).

2211-2855/$ - see front matter © 2013 Elsevier Ltd. All rights reserved.
http://dx.doi.org/10.1016/j.nanoen.2013.01.007

performance is important for applications such as electronics, transportation, and others where space is limited [7,8].

Many highly porous carbon materials have relatively low bulk densities of less than 0.5 g/cm^3 [8]. Typically, activated carbons have densities of about 0.5 g/cm^3 and reported volumetric capacitances in the range of 50 to 80 F/cm^3 [9]. CDC films with a thickness of ~50 μm were reported to have a volumetric capacitance of about 60 F/cm^3, while values of ~160 F/cm^3 have been reported for CDC films with a thickness of ~2 μm [4].

Previously, our group reported the synthesis of a new carbon material that was prepared by the activation of microwave-exfoliated graphite oxide ('MEGO'). Activated MEGO ('a-MEGO') was found to have a high electrical conductivity, a low O and H content, and a structure composed of nearly 100% sp^2-bonded carbon [10]; it exhibited a Brunauer–Emmett–Teller (BET) [11] specific surface area (SSA) of up to 3100 m^2/g and a large pore volume with pore sizes ranging from less than 1 nm to ~5 nm. Supercapacitors with a-MEGO electrodes demonstrated a high gravimetric capacitance of 166 F/g in ionic liquid electrolytes such as 1-butyl-3-methyl-imidazolium tetrafluoroborate (BMIM BF_4) in acetonitrile (AN) [11]. But a low volumetric capacitance of 60 F/cm^3 was obtained due to the low density (~0.3 g/cm^3) of the as-made a-MEGO electrode.

By simply compressing the as-made a-MEGO, a volumetric capacitance as high as 110 F/cm^3 was obtained in a BMIM BF_4/AN electrolyte. This improved volumetric capacitance is attributed to the higher density and smaller pore size of the a-MEGO electrodes after compression.

Experimental

The synthesis of a-MEGO was described in our previous report. [10] Briefly, MEGO was prepared from graphite oxide (GO) by microwave irradiation, [12] then activated with KOH at 800 °C in a tube furnace. Electrodes of a-MEGO were prepared using best practice methods [13]. 5 wt% Polytetrafluoroethylene (PTFE; 60 wt% dispersion in water) was added to the a-MEGO powder (SSA ~2600 m^2/g) as a binder. The mixture of a-MEGO and PTFE was ground up with mortar and pestle, rolled into 120 μm thick raw films and punched into 1.1 cm diameter electrodes. Electrodes with thicknesses of 60 μm were made following the standard rolling method, yielding the '*uncompressed* sample'. To increase the density, separate raw films were placed in a 13 mm KBr Die Set (International Crystal Laboratories) and compressed using a hydraulic press. Two types of compressed samples were separately made using 10 t (*compressed*-10, 72 μm thick) and 25 t (*compressed*-25, 57 μm thick) of compression force.

The BET SSA and the pore size distribution (PSD) of the uncompressed and compressed electrodes were obtained from N_2 adsorption isotherms (Micromeritics ASAP 2020). The electrical conductivity of these samples was measured using a four probe setup. To measure the supercapacitor performance, the electrodes were configured in a two-electrode test cell consisting of two current collectors, two electrodes, and a porous separator (Celgard® 3501) supported in a test fixture consisting of two stainless steel plates [13]. A conductive carbon-coated aluminum foil (Exopack™ 0.5 mm thick, 2-sided coating) was used with BMIM BF_4/AN and tetraethylammonium tetrafluoroborate (TEA BF_4) in acetonitrile (TEA BF_4/AN) electrolytes, respectively.

Results and discussion

The density and specific surface area of the a-MEGO electrodes before and after compression are shown in Table 1. The density of the uncompressed electrode was determined to be 0.34 g/cm^3. By applying a force of 10 t, the density of the *compressed*-10 sample was 0.61 g/cm^3. A second sample was made by applying a force of 25 t, yielding a density of 0.75 g/cm^3 (*compressed*-25). The BET SSA of the *compressed*-10 sample was 1560 m^2/g, compared to 1380 m^2/g in the *uncompressed* sample. The adsorption data shown in Figure 1 suggest that this increase in SSA is due to a larger contribution from micropores following the first compression. Further compression resulted in a sharp decrease in the SSA to 710 m^2/g. The BET SSA measurements and pore size estimates were obtained based on high resolution, low pressure adsorption/desorption experiments with nitrogen (77.4 K) and non-local density functional theory (NLDFT) calculations. The uncompressed electrode exhibited an isotherm similar to that of a-MEGO powder [10] (shown in Figure S1). While the adsorption volume at lower pressure of the *compressed*-10 electrodes increased, a sharp decrease of the nitrogen uptake was observed for the

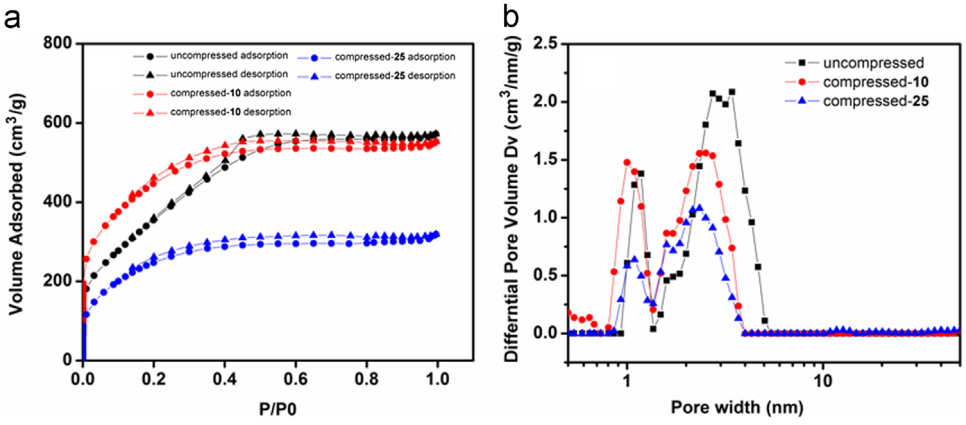

Figure 1 (a) High-resolution, low-pressure N_2 (77.4 K) adsorption–desorption isotherms of uncompressed and compressed electrodes, and (b) pore size distribution for N_2 (calculated from the data using a slit/cylindrical NLDFT model).

compressed-25 electrodes. The pore size distribution shown in Figure 1(b) suggests that the volume of the mesopores in the as-made electrodes, with an average size of ~4 nm, was decreased by compression and the peak of the mesopores shifted closer to ~2 nm. At the same time, the volume of ~1 nm micropores showed a slight increase for the sample compressed with 10 t, but reduced dramatically for the sample compressed with 25 t. The adsorption studies suggest that most of the mesopores either collapsed or were compressed down to the size range of the micropores. (The low resolution isotherm and PSD of as-made a-MEGO powder with BET SSA of 2600 cm^2/g is shown in the Supporting Information.) The DC conductivity varied with the compression force, measuring 0.15 S/cm for the *uncompressed* sample, 2.13 S/cm for the *compressed*-10 sample, and 1.74 S/cm for the *compressed*-25 sample. The increase in conductivity is likely due to void removal from compression and increased interparticle contact area.

The electrochemical performance of both uncompressed and compressed electrodes was tested with cyclic voltammetry (CV), constant current (CC) galvanostatic charge-discharge, and frequency response analysis (FRA). The specific capacitances from CC and those from CV at a scan rate of 100 mV/s (from 0 to 3.5 V) are shown in Table 1. The gravimetric capacitance from CC remained almost unchanged for the sample compressed with 10 t, and slightly dropped to 147 F/g after compression with 25 t. Due to the density increase, the *compressed*-25 sample had a volumetric capacitance of 110 F/cm^3 in BMIM BF_4/AN electrolyte. In TEA BF4/AN electrolyte, the volumetric capacitance of the *compressed*-25 sample was 98 F/cm^3. This volumetric capacitance is to our knowledge higher than all of the activated carbons in the literature (for IL or organic electrolytes) and is comparable to that of the CDC coating with a thickness of 20 μm [4]. However, the gravimetric capacitance calculated from the CV at 100 mV/s scan rate in Figure 2 strongly depends on the load used in the compression. CV studies (shown in Figure S3) on the gravimetric capacitance of the compressed samples show it also decreased when the scan rate was increased. The gravimetric and volumetric energy densities were calculated based on the capacitance values from the CC curves, and the results are provided in Table 1. A high volumetric energy density of 48 Wh/l (normalized to the volume of the two carbon electrodes) was obtained from the *compressed*-25 sample in the BMIM BF_4/AN electrolyte.

Although the gravimetric capacitance from CC testing was almost unchanged after compression, the supercapacitor performance was affected. As seen in Figure 2(a), the CV curves (at 100 mV/s) of the compressed samples are not as rectangular as that of the uncompressed a-MEGO electrodes. Also, the CV curves (Figure S2) of the compressed samples were slightly distorted (while the CV curves of the uncompressed sample were not) when the scan rate was increased from 20 mV/s to 100 mV/s, indicating a slower charge propagation of the ions at the higher scan rates for the compressed samples. In addition, the resistance drop at the beginning of the discharge curve (Figure 2(b)) increased from 3.4 Ω for the *uncompressed* electrode, to 10.2 Ω (*compressed*-10) electrode and to 13.4 Ω (*compressed*-25) electrode. As a result, the volumetric power density decreased from 79 kW/l for the *uncompressed* sample to

Table 1 Comparison of a-MEGO electrode performance metrics before and after compression.

Sample	Density (g/cm^3)	BET SSA (m^2/g)	Galvanostatic charge-discharge (F/g)	Cyclic voltammetry (F/g)	Volumetric capacitance (F/cm^3)	Gravimetric energy density (Wh/kg)	Volumetric energy density (Wh/l)
				100 mV/s			
Uncompressed	0.34	1382	159 @ 1.33 A/g	149	54	68	23
Compressed-10	0.61	1556	158 @ 1.22 A/g	120	96	67	41
Compressed-25	0.75	707	147 @ 1.24 A/g	110	110	63	48

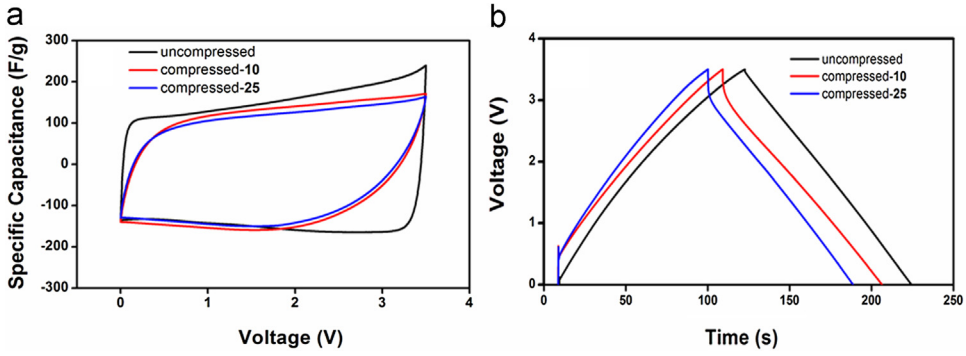

Figure 2 Electrochemical testing in BMIM BF_4/AN electrolyte: (a) CV curves at 100 mV/s for the uncompressed and compressed electrodes, and (b) galvanostatic charge-discharge curves for the uncompressed and compressed electrodes.

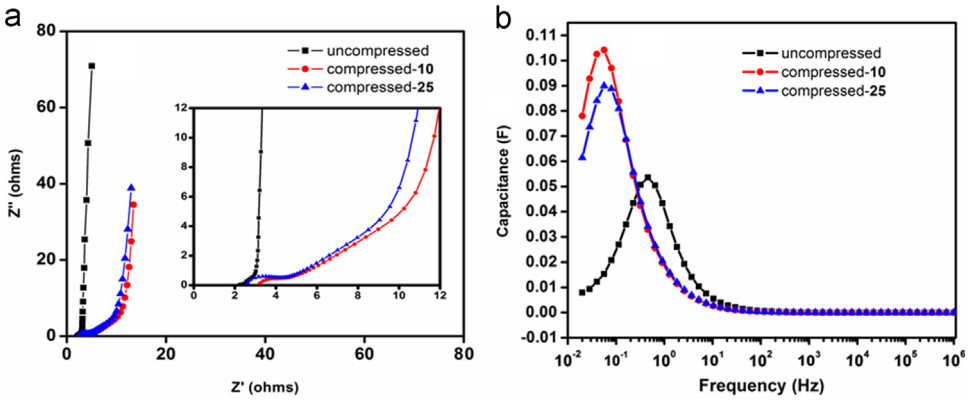

Figure 3 (a) Nyquist plots from the frequency response analysis. Inset magnifies the data in the high frequency range, and (b) evolution of imaginary capacitance versus frequency for cells with uncompressed and compressed electrodes.

17 kW/l for the *compressed*-25 sample. In TEA BF4/AN electrolyte, the CV curves of both *uncompressed* and *compressed* samples remained rather rectangular and the resistance drop at the beginning of the discharge curve showed small variation between the electrodes (5 Ω for the *uncompressed* electrode to 4.3 Ω for the *compressed*-25 electrode) (Figure S2). This indicated better charge propagation in TEA BF4/AN electrolyte. Therefore, the volumetric power density, which is a function of voltage and resistance, increased with the density of the electrode from 31 kW/l for the *uncompressed* sample to 37 kW/l for the *compressed*-25 sample. The Ragone plot with volumetric energy and power density values is provided in Figure S4.

The kinetics of ion transport in both uncompressed and compressed electrodes in BMIM BF_4/AN was further investigated using electrochemical impedance spectroscopy (EIS) with a frequency range from 0.01 Hz to 1 MHz. The EIS results were analyzed using Nyquist plots, shown in Figure 3(a). The steep slopes of the curves in the low frequency region of all three electrodes suggest nearly ideal capacitive behavior of the cells. The mid-high frequency 45° slope portion of the Nyquist plots, which is usually modeled by a de Levi transmission line, is due to the transport of ions in cylindrical pores [14]. It should be noted that this 45° slope portion is not a result of Warburg diffusion (unrestricted semi-infinite linear diffusion to a large planar electrode). The high frequency region for the *uncompressed* electrode compared to that of the two compressed electrodes indicates a lower electrode resistivity. The total equivalent series resistance (ESR) was estimated to be 3.1, 8.3, and 9.4 Ω for the *uncompressed*, *compressed*-10, and *compressed*-25 electrodes, respectively. These values are similar to those obtained from CC testing. The increased ESR of the compressed electrodes is likely due to the collapse of the large mesopores. Figure 3(b) presents the evolution of the imaginary part of the capacitance versus frequency where the relaxation time constant τ_0 of the cell is the reciprocal of the frequency f_0 at the peak. [15] The results indicate that the cell with the uncompressed electrode (τ_0=2.2 s) is able to deliver its stored energy faster than that of cells with the compressed electrodes (τ_0=10 s) [16]. We surmise this is due to the pore size distribution of the samples as large mesopores are more important for fast ion diffusion in porous electrodes.

Conclusion

By applying a compressive force (10 t or 25 t) to as-made a-MEGO electrodes, the volumetric capacitance and volumetric energy density of a-MEGO based supercapacitors were increased from 60 F/cm^3 and 23 Wh/l to 110 F/cm^3 and 48 Wh/l, respectively. This is largely due to a higher density of the compressed a-MEGO samples, which also predominately contain micropores smaller than 2 nm. A fraction of the mesopores present in the uncompressed a-MEGO collapse from the compression, leading to a higher equivalent series resistance and thus a lower power density (on a gravimetric basis) of the compressed versus the uncompressed electrodes (but the compressed samples have higher power density on a volumetric basis). Our study suggests that, as with activated carbons used as electrodes in supercapacitors, the micropores in a-MEGO are primarily responsible for charge storage while the mesopores provide fast ion transport channels for the ionic liquid electrolyte (BMIM BF_4/AN) or organic electrolyte (TEA BF_4/AN) used in the study here.

Acknowledgment

We appreciate funding support from the U.S. Department of Energy (DOE) under Award DE-SC0001951. Y. Lu and Y. Zhu appreciate support from the National Basic Research Program of China with Award no. 2012CB922001.

Appendix A. Supporting information

Supplementary information associated with this article can be found in the online version at http://dx.doi.org/10.1016/j.nanoen.2013.01.007.

References

[1] J.R. Miller, P. Simon, Science 321 (5889) (2008) 651–652.
[2] O. Barbieri, M. Hahn, A. Herzog, R. Kotz, Carbon 43 (6) (2005) 1303–1310.
[3] C. Portet, G. Yushin, Y. Gogotsi, Carbon 45 (13) (2007) 2511–2518.
[4] J. Chmiola, C. Largeot, P.L. Taberna, P. Simon, Y. Gogotsi, Science 328 (5977) (2010) 480–483.

[5] A. Izadi-Najafabadi, S. Yasuda, K. Kobashi, T. Yamada, D.N. Futaba, H. Hatori, M. Yumura, S. Iijima, K. Hata, Advanced Materials 22 (35) (2010) E235–E241.
[6] M.D. Stoller, S. Park, Y. Zhu, J. An, R.S. Ruoff, Nano Letters 8 (10) (2008) 3498–3502.
[7] E. Frackowiak, F. Béguin, in: M. Lu (Ed.), Supercapacitors (New Materials for Sustainable Energy and Development), 1st ed., Wiley-VCH, New York, 2013, p. 538.
[8] Y. Gogotsi, P. Simon, Science 334 (6058) (2011) 917–918.
[9] P. Simon, Y. Gogotsi, Accounts of Chemical Research, in press.
[10] Y. Zhu, S. Murali, M.D. Stoller, K.J. Ganesh, W. Cai, P.J. Ferreira, A. Pirkle, R.M. Wallace, K.A. Cychosz, M. Thommes, D. Su, E.A. Stach, R.S. Ruoff, Science 332 (6037) (2011) 1537–1541.
[11] S. Brunauer, P.H. Emmett, E. Teller, Journal of the American Chemical Society 60 (2) (1938) 309–319.
[12] Y. Zhu, S. Murali, M.D. Stoller, A. Velamakanni, R.D. Piner, R.S. Ruoff, Carbon 48 (7) (2010) 2118–2122.
[13] M.D. Stoller, R.S. Ruoff, Energy and Environmental Science 3 (9) (2010) 1294–1301.
[14] R. De Levie, Advances in Electrochemistry And Electrochemical Engineering, in: P. Delahay (Ed.), Electrochemistry, vol. 6, John Wiley & Sons, New York, 1967.
[15] P.L. Taberna, C. Portet, P. Simon, Applied Physics A: Materials Science and Processing 82 (4) (2006) 639–646.
[16] P.L. Taberna, P. Simon, J.F. Fauvarque, Journal of the Electrochemical Society 150 (3) (2003) A292–A300.

Shanthi Murali received her Ph.D. in Materials Science and Engineering from The University of Texas at Austin in 2012, under the direction of Prof. Rodney S. Ruoff. Her Ph.D. thesis included investigation of reduction of exfoliated graphite oxide, and energy storage in systems with graphene-based materials as the electrodes. She received her M.S. in Chemical Engineering from Auburn University in 2008 where her thesis work involved liquid crystalline assembly of nanowires. During her Ph.D. studies, she worked as a research intern in Intel Labs. She currently works for iRunway Inc., a technology consulting firm in Austin, Texas.

Neil Quarles received his B.S. in Mechanical Engineering from The University of Texas at Austin in December, 2012. As an undergraduate research assistant, he worked with Dr. Shanthi Murali and Dr. Meryl Stoller in Prof. Rodney S. Ruoff's group. He has assisted primarily in research involving ultracapacitors and lithium-ion batteries, including the use of graphene-based materials as electrodes, as well as the development of testing techniques for cells.

Li Li Zhang received her B. Eng. in Chemical and Biomolecular Engineering from the National University of Singapore in 2004. After two years industrial experiences in Micron, she continued her Ph.D. study in the same department at the National University of Singapore from 2006 and received her Ph.D. degree in 2011. She worked as a research engineer from 2010 to 2011 at NUS. She now works in Professor Ruoff's group as a postdoctoral research fellow at The University of Texas at Austin. Her research interest is developing high-performance energy storage materials and systems.

Jeffrey R. Potts is a Scientist at Baker Hughes in Houston, Texas. He completed his PhD in Materials Science & Engineering at the University of Texas at Austin in 2012 under the direction of Rodney S. Ruoff, and earned a B.S. in Mechanical Engineering from Oklahoma State University in 2008. During his PhD studies, he worked as a research intern at Sandia National Laboratories in Albuquerque, New Mexico and collaborated closely with Goodyear Tire & Rubber Company on elastomer nanocomposites research. To date, he has authored or co-authored 16 papers on polymer nanocomposites and graphene-based materials.

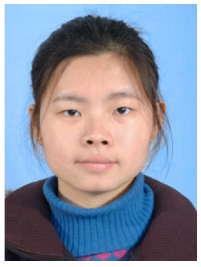

Ziqi Tanreceived her B.S. in Materials Physics from Hefei University of Technology in China in 2011. She is currently a postgraduate supervised by Professor Yanwu Zhu and Professor Yalin Lu in University of Science and Technology of China. Her research is focused on the novel carbon electrode materials for the application in supercapacitors.

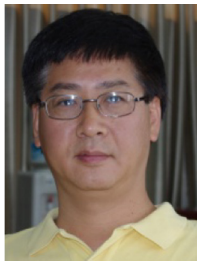

Yalin Lucurrently is the Executive Head of Materials Science and Engineering Department and the Director of CAS key Laboratory of Materials for Energy Conversionat University of Science and Technology of China. He obtained his Ph.D in Solid State Physics from Nanjing University in China in 1991. His research group works on energy materials, THz technology and metamaterials, nonlinear optics, electro-optics, and lasers, thin film growth and materials physics of complex oxides.

Yanwu Zhu joined University of Science and Technology of China in 2011 as a professor. His Ph.D is in condensed matter physics from National University of Singapore (2007). He was working as a postdoctoral fellow in the National University of Singapore Nanoscience & Nanotechnology Initiative (2007–08) and in the Department of Mechanical Engineering at The University of Texas at Austin (2008–2011). He has co-authored more than 90 peer-reviewed papers. His current research includes carbon nanomaterials for efficient energy storage and conversion.

Rodney S. Ruoff joined The University of Texas at Austin as a Cockrell Family Regents endowed chair in September, 2007. His Ph.D. is in Chemical Physics from the University of Illinois-Urbana (1988) and he was a Fulbright Fellow in 1988–89 at the Max Planck Institute fuerStroemungsforschung in Germany. He was the John Evans Professor of Nanoengineering at Northwestern University and director of NU's Biologically Inspired Materials Institute from 2002–2007. He has co-authored 340 peer-reviewed publications devoted to materials science, chemistry, physics, mechanics, engineering, and biomedical science. He is a Fellow of the MRS, APS, and the AAAS.